Korean Journal of Remote Sensing, Vol.22, No.1, 2006, pp.11~24

Surface Heat Flux and Oceanic Heat Advection in Sendai Bay

Chan-Su Yang*† and Kimio Hanawa**

Ocean Satellite Research Group, KORDI, Ansan-city 237-0061, Korea*

Department of Geophysics, Tohoku University, Sendai 980-8578, Japan**

Abstract : Coastal sea surface temperature (CSST) and meteorological data from January through December 1995 are used to estimate the net surface heat flux and heat content for Sendai Bay. The average annual surface heat flux in the area north of the bay is estimated to be +35 W m^{-2}, whereas the southwestern area is estimated to be +56 W m^{-2}. Therefore, the net surface heat flux shows a net gain of heat over the whole bay. The largest heat gain occurs near Matsukawaura, where the strong Kuroshio/Oyashio interaction produces anomalously cold SST and wind is more moderate than in other regions of Sendai Bay over most of the year. The lowest heat gain occurs around Tashiro Island, where the temperature difference between air and sea surface is lower and wind is stronger. The heat budget shows that both surface forcing and horizontal advection are potentially important contributors to the seasonal evolution of CSST in the bay. From the AVHRR and SeaWiFS data, it is found that offshore conditions between the bay and Eno Island are different due to the presence of the Ojika Peninsula. It is also shown that the temporal behaviors of SSTs in the bay are closely connected with the air-sea heat flux and offshore conditions.

Key Words : AVHRR image, SeaWiFS image, sea surface temperature (SST), Kuroshio, Oyashio, heat flux.

1. Introduction

The ocean-atmosphere heat system is basically driven by radiation of the sun. There are essential processes those determine how the atmosphere and ocean respond to the received energy. The sea surface temperature (SST) plays a significant role in the exchange of heat between the ocean and atmosphere. The outgoing longwave radiation as well as the sensible (conductive) and latent (evaporative) heat fluxes are all a function of SST. These fluxes in combination with the incoming short-wave radiation determine the net air-sea heat exchange. This exchange is important both for regulating climate as well as for establishing thermohaline circulation in the ocean, which is of particular interest in marginal and semi-enclosed seas.

The research area, Sanriku Coast and Sendai Bay in the northeastern region of Japan (Figure 1) is characterized by rias coast and by mountain ranges located near the coastal area, but the inner shore of Sendai Bay occupies a comparatively wide plain. In the Kuroshio/Oyashio Frontal Region (Figure 1), SST patterns are largely determined by spatial variations

Received 4 November 2005; Accepted 7 February 2006.

† Corresponding Author: C. – S. Yang (yangcs@kordi.re.kr)

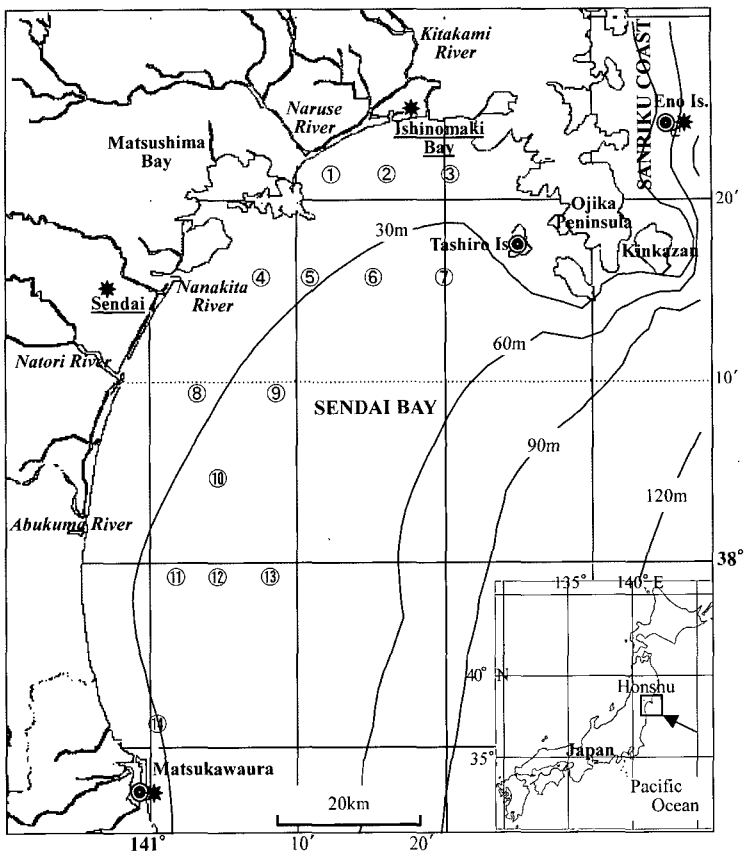

Fig. 1. Map of Sendai Bay. The circled number, enclosed circle and star denote the measurement locations; ⓝ = temperature profile, ◉ = coastal SST, ✸ = meteorological data.

in the strength of three currents: the Kuroshio, Oyashio, and Tsugaru Warm Current (Nagata *et al.*, 1978; Hanawa, 1983; Hanawa, 1995; Yang *et al.*, 1999). Hanawa (1983) monitored SST in and around Sendai Bay by ferry and confirmed the importance of the Tsugaru Warm Current (TWC) and Oyashio water in changing SST on seasonal scales. Despite small spatial scale SST changes in the "heating" season (June to August), dramatic SST drop in the bay occur in winter (November to February), as compared with the Sanriku Coast. In the research area, peninsula and several islands restrict water flow between the relatively shallow inner basin and outer region, creating a persistent pool of different water which is evident both in salinity and in satellite infrared and chlorophyll imagery (Yang *et al.*, 1999a; Yang *et al.*, 1999b; Yang, 2000a). Sendai Bay is also subject to strong atmospheric forcing. Isolated from the moderating influence of the Pacific Ocean by a continuous chain of mountains along the Ojika peninsula, the bay exhibits the strongest SST variability of any region in the northwestern Pacific coastal region between 31.8°N and 38.4°N (Yang *et al.*, 2000; Yang, 2000b; Yang *et al.*, 2001).

Nagata *et al.* (1978) analyzed SST in the coastal region of northeast Japan and concluded that SST is higher in December than in May along the Sanriku coast due to its offshore variability. As a result, this

region is easily affected by variations in its offshore environment and weather conditions.

In the present study, our goal is to seek the cause of SST changes observed in and near Sendai Bay and, in particular, in the months of May and December. In this paper we focus on a seasonal cycle of water temperature, including its regional variability, around Sendai Bay, and aim to explain the seasonal oscillation in this region based on consideration of the heat flux and offshore conditions. We also examine what is important to the order of magnitude of SST in and around Sendai Bay, the predominant feature of Sendai Bay temperature field, and how that feature is formed.

This paper is organized as follows. First the SST and meteorological data are presented and the seasonal variability of the atmosphere and surface temperature around the bay are described. Next, estimates of the various heat flux components are performed, and their spatial and temporal behaviors are compared with that obtained for the open ocean by Iwasaka and Hanawa (1990). The net heat flux is then calculated, and the relationship between net heat flux and the seasonal pattern of SST is discussed. Finally, satellite images are described and presented as clear evidence of flow pattern of the Kuroshio/ Oyashio Currents.

2. Data

Meteorological variables are measured at four locations in and around Sendai Bay by the automated meteorological data acquisition system (AMeDAS) of the Japan Meteorological Agency (Figure 1). SSTs are measured at Eno Island and Tashiro Island by the Miyagi Fisheries Research Center, and at Matsukawaura by the Fukushima Fisheries Research Center (Figure 1). Coastal SST (CSST) and meteorological data from January through December 1995 are used to estimate the net surface heat flux and advection transport (heat content) for Sendai Bay. Monthly means of these data are collected for the period of 1990-1997. The approximate elevations of the sites are Matsukawaura (9m), Sendai (39m), Ishinomaki (43m), and Eno Island (40m). Eno Island and Matsukawaura stations measure wind speed and direction, air temperature, and SST, but only SSTs are measured at Tashiro Island.

The AVHRR data consist of 1.1-km pixel resolution, 11-μm channel brightness temperatures from NOAA 11 and NOAA 14 data. Ratio of successful detection of the surface Kuroshio/Oyashio Front is very low (0.17%, 53 scenes out of 310), because most of the image is covered with cloud. In addition, since thin clouds shroud the underlying water from analysis, monthly mean images are used to reduce the effects of cloud. Furthermore, there are two reasons why the months of May and December are mainly used; (1) images in summer are not even if there is no cloud cover because the surface temperatures are almost uniform in space, (2) in Sendai, which is located on the Pacific coast, the overcast condition prevails in summer and fall every year. Fifty-three cloud-free AVHRR images, taken in the months of May and December between 1990 and 1994, were used for this study.

The satellite OrbView-2 carried an instrument known as the Sea-viewing Wide Field-of-view Sensor (SeaWiFS), which measures the color of water in six visible spectral bands, as well as two near-infrared bands. SeaWiFS sensors operating within visible wavelengths can relay useful chlorophyll-a information only when there is no cloud. This information is very useful to detect the surface Kuroshio/Oyashio Front in the area of present study.

1) Seasonal Variations of SST in the Sendai Bay and Sanriku Coast

Sendai Bay has high SST ranges of nearly 17°C over the entire year (Figure 2). However, Eno Island station, located just outside the bay, has much less seasonal variation than inside the bay. Seasonal SST variability is the highest at Matsukawaura as shown in Figure 2. There are also clear tendency in temporal behaviors of SST at three stations; (1) SST orders at Matsukawaura and Eno Island are changed in April and November, (2) at Eno Island temperature is higher by about 2.7°C in December than in May.

2) Atmospheric Conditions in Monthly Mean Climatologies

Plots of the available meteorological and saline data are presented as monthly averages in Figure 3. Seasonal variation of air temperature is fairly similar at the various stations, with a maximum difference of 2°C. In addition, temporal behaviors of air temperature at Matsukawaura and Eno Island occur in the order shown in Figure 2, but turning points of temperature occur in April and October. The minimum occurs in February at Eno Island, and January at Matsukawaura and Tashiro Island, whereas the maximum occurs in August at all stations. Based on Figures 2 and 3, it can be considered that the atmosphere-ocean interaction is strongly derived, although this area belongs to the coastal region.

The inner shore of Sendai Bay occupies a comparative wide plain, but mountain ranges are located near the coast area of Sanriku and west of Matsukawaura (Figure 1). These mountains tend to channel winds along the ground in the vicinity of the bay. During the summer, winds blow predominantly from the southeast and northeast, bringing cold, moist

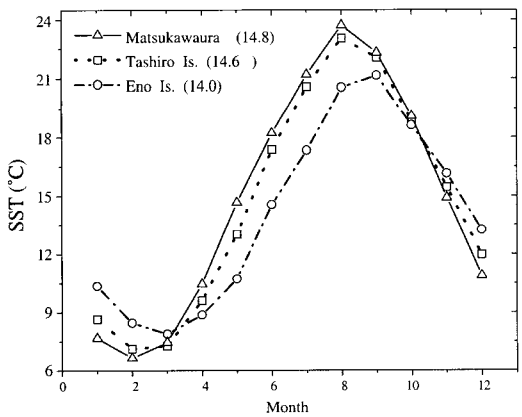

Fig. 2. Seasonal changes of SST at three stations during the 1990-1997. Parenthesis of index indicates the annual average (°C).

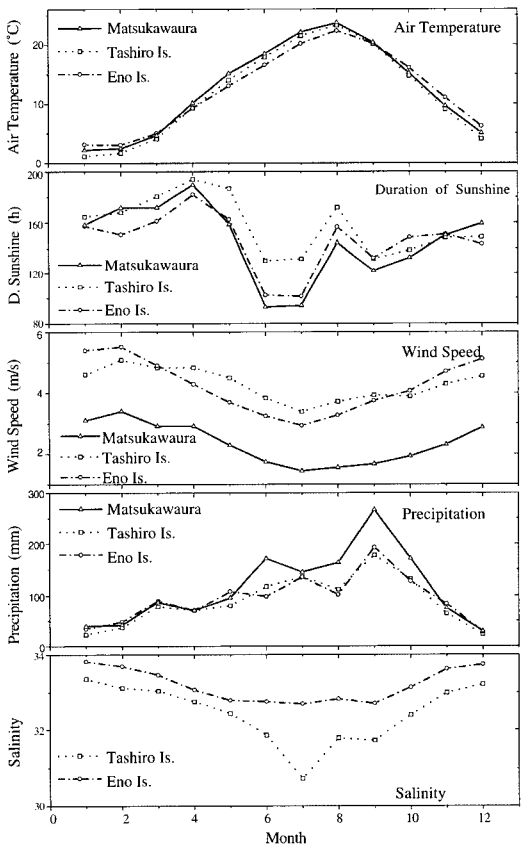

Fig. 3. Monthly averaged surface meteorological variables and salinity at each station during the 1990-1997: air temperature, duration of sunshine, wind speed, precipitation, and salinity (from the top to bottom panels).

Pacific air into the bay. During the rest of the year, winds have a rather wide range in direction from the southwest to the northwest at Matsukawaura, while at other areas the wind tends distinctly to blow out of the northwest (strictly speaking, NNW). Winds measured at Eno and Tashiro Islands are almost twice as strong as those measured at Matsukawaura. In addition, winter wind speeds are approximately twice those in summer except the Tashiro station, which shows relatively low seasonal variation. High wind speed results in relatively high evaporation rates over the northern bay.

Seasonality is also apparent in the duration of sunshine, precipitation, and salinity. Duration of sunshine and salinity are the smallest in summer, but the minimum of precipitation occurs in winter. Precipitation for Matsukawaura shows a pronounced annual cycle with a maximum during September (Figure 3). Duration of sunshine is much longer in Tashiro Island than at other stations, but its salinity is much smaller than Eno Island. The inner bay, that is, is mainly affected by many rivers, even if the mouth of the bay is opened to the southeast. It appears in general that in seasonal variations, significant differences between all stations occur owing to a slight difference in orographical factor. In addition, meteorological variables shown in Figure 3 also reflect the climate system of this region: 1) existence of Bai-u Front from June to August, 2) Akisame Front in September.

Figure 4 shows plots of the difference between air temperature and SST (hereinafter referred to as T_a-T_s) at three stations in and around Sendai Bay. Most of the stations are dissimilar in value except during March and April. In the bay, Matsukawaura and Tashiro Island show similar trends in T_a-T_s from March to October. Although air temperature and SST during 1990-1997 are higher at Matsukawaura than for Tashiro Island, the annual average of SST is

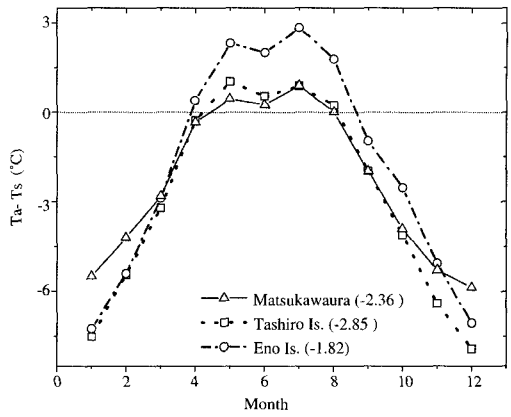

Fig. 4. Monthly difference between air temperature (T_a) and SST (T_s) at three meteorological stations during the 1990-1997. Numeral in the parenthesis of index indicates the annual average (°C).

almost uniform over the bay, within 0.2°C difference. Therefore, it is possible that the Tashiro T_a-T_s represents larger values during winter as shown in Figure 4.

3. Heat Flux

1) Surface Heat Flux

(1) Heat flux calculations

The aerodynamic bulk method is the only practical technique available to estimate surface heat fluxes from readily available meteorological data (Iwasaka and Hanawa, 1990; Kizu, 1998). Estimates of the surface heat flux were made from monthly mean values of wind speed, temperature, cloud cover, relative humidity, and sea level and atmospheric pressure using the same formulas as Lavin and Organista (1988). The incident solar radiation was estimated using Reed's (1977) formula, which is commonly used by the oceanographic community (Gill, 1982; Lavin and Organista, 1988; Iwasaka and Hanawa, 1990; Paden *et al.*, 1993; Castro *et al.*, 1994;

Kizu, 1998). The sensible and latent heat fluxes were estimated from the bulk aerodynamic formulas using exchange coefficients dependent upon the wind speed and the air-sea temperature difference (Bunker, 1976). The net longwave radiation was estimated from the SSTs using the formula modified for cloud cover (Reed, 1976, 1983). Details of each formula used in the present study are described in the Appendix.

Lavin and Organista (1988) have shown that estimates of the various heat flux components made using monthly averaged meteorological data generally have an error of less than 10% when compared with estimates made using daily averaged meteorological data. The heat flux near Ishinomaki, therefore, is estimated from the daily mean data, but since the number of observations is insufficient, monthly mean values are used at Matsukawaura.

(2) Temporal and spatial variabilities of the surface heat flux

Available meteorological data are presented in Figure 5 and show the regional (North - South) differences between Ishinomaki and Sendai. Time series of the various components of the surface heat flux are presented in Figure 6 with positive values indicative of a heat gain by the ocean. These values represent the fluxes for the region north and south of the Kinkazan-Matsukawaura line, the mouth of the bay, corresponding to the area for which bounds of Sendai Bay is generally estimated.

The temporal behaviors of the various heat flux components are similar. The incident solar radiation, calculated at 38.4°N and 38.2°N , has a maximum in July and minimum in March with a net annual average of + 152 W m^{-2} (the northern region) and + 150 W m^{-2} (the southern region) in the 1995 period. The latent heat flux of the north shows a minimum value in July and a maximum in November,

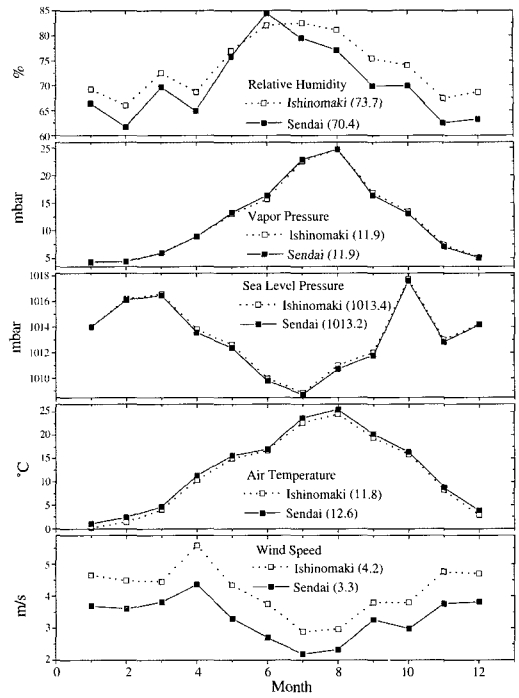

Fig. 5. Monthly-averaged meteorological data at Sendai and Ishinomaki stations during 1995: sea level pressure, air temperature, wind speed, vapor pressure, and relative humidity (from the top to bottom panels). Numeral in the parenthesis of index indicates the annual average.

compared to June and November, respectively, for the Matsukawaura analysis. The average annual latent heat flux of the north was slightly higher for the 1995 data set, with a net loss of 55 W m^{-2} and an evaporation rate of 0.75 m yr^{-1} compared with the 51 W m^{-2} and an evaporation rate of 0.51 m yr^{-1} estimated at Matsukawaura. The back (net longwave) radiation has also seasonality, with a minimum in summer due to the increase in water vapor content of the lower atmosphere. Cloud cover further reduces the back radiation during the summer as well as in all months in the 1995 analysis yielding a net loss of approximately 35 W m^{-2} and 33 W m^{-2} over the year at the north and south, respectively. The sensible heat flux at Ishinomaki shows a net annual heat loss of approximately 27 W m^{-2} compared with 11 W m^{-2}

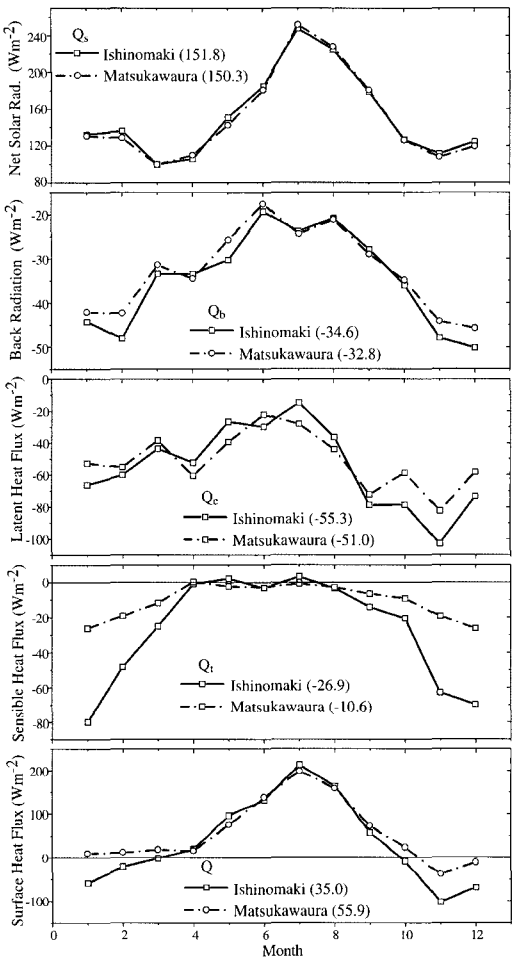

Fig. 6. Monthly averaged surface heat fluxes for the region of Ishinomaki and Matsukawaura during 1995. Numeral in the parenthesis of index indicates the annual average.

for Matsukawaura.

The total net surface heat flux (Figure 6) north of the Kinkazan-Matsukawaura line shows a net heat gain by the ocean from April through September, and a net heat loss from October through March. The estimated net annual surface heat flux is +35 W m^{-2} for Ishinomaki. On the other hand, we use the same surface heat flux formulae to estimate a net surface heat flux of +56 W m^{-2} over the southern basin, with heat loss occurring only in the months of November and December. Kizu (1998) has studied the monthly mean insolation in the Sea of East/Japan coast, near 37.5°N, which is located at similar latitude with Sendai. Minimum values of estimated insolation in Sendai have been observed to be higher approximately by 30 W m^{-2} than that of the Sea of East/Japan coast.

The large heat flux difference between the areas north and south of Sendai Bay in the present study may seem to relate to the difference of humidity in the two data sets. During 1995, the Ishinomaki humidity shows essentially seasonal variation with a relatively high mean of 74% and a range of 66-83%. Humidity, however, measured at the Sendai station averaged 70% and ranged from 62% in winter to 84% in summer. The interannual variability in humidity may occur in response to large-scale climatic variability over the Pacific Ocean or may be related to the strength of the atmospheric pressure systems over the North Pacific (Paden *et al.*, 1993). In this region, however, a strong seasonal cycle seems to occur, with a high mean and low interannual variation during 1990-1998, while the Sendai humidities have large interannual variation. As a result, the difference between humidities at two stations can be not relevant in the spatial variability of the heat flux in the bay.

In the north a local minimum in the heat flux occurs over the shallow shelf on the inside of the bay (near the coast). In general, however, the heat flux is hypothesized to be fairly uniform over most of the inner basin, where SSTs are consistently preserved over the year, with a small standard deviation of 0.89°C compared with 1.03°C farther offshore. The difference between these results is due to wide differences between air temperature and SST as shown in Figure 4. Although air temperature and SST during 1990-1997 are higher at Matsukawaura than at Tashiro Island, the annual average of SST is almost uniform over the bay within 0.2°C difference. The Tashiro T_a-T_s represents larger values during winter.

In addition, since wind speeds measured at Ishinomaki are also much higher than those at Matsukawaura, the heat loss is larger during winter at the coast near Ishinomaki. Consequently, it is shown that the temporal behaviors of SSTs in the bay (Figure 2) are closely connected with the air-sea heat flux.

Although all the heat flux components of Tashiro Island are larger than the Matsukawaura, the spatial pattern of the net surface heat flux is primarily determined by the pattern of the sensible heat flux. The back radiation and latent heat flux do not vary much in space, ranging from -5.7 to +1.1 W m^{-2} and -20.6 to +13.4 W m^{-2}, respectively. The sensible heat flux, on the other hand, ranges from 3 to -80 W m^{-2} at Ishinomaki to as low as 0 to -26 W m^{-2} in Matsukawaura, with a minimum in winter at both sides.

Bowen ratio of Matsukawaura (0.2) is similar to that calculated for farther offshore by Iwasaka and Hanawa (1990), but the value (0.5) at Ishinomaki is higher. This means that the situation at Matsukawaura is similar to that in the open ocean.

In general, the heat loss, in conjunction with evaporation, produces a warm, saline water mass, which flows out of the bay in exchange for cold, relatively fresh water at depth. In the northern region, since there are the freshwater flux of two-thirds as much as the total volume (0.73 km^3/month) due to many rivers, this freshwater is dispersed by local or large-scale circulation and mixed with the bay water, reducing surface temperatures over the most of the northern bay except during the spring. The evaporation rate, therefore, falls under what was expected, below 1 m yr^{-1}. This heat gain is opposite to that estimated in the open ocean, which loses heat to the atmosphere on an annual average (Iwasaka and Hanawa, 1990).

In the southern region, the SSTs near Matsukawaura reduced by Kuroshio/Oyashio exchange can have a large impact on the surface heat flux by lowering the saturation vapor pressure of the air. Heated surface waters are mixed downward, pumping heat deep into the water column, where it is less able to interact with the atmosphere. The air overlying the sea surface is cooled and therefore retains less moisture. As a result, evaporation and the associated latent heat loss are reduced. The latent heat flux in the bay appears to be only half of that estimated by Iwasaka and Hanawa (1990) for the open ocean. When the latent heat flux associated with the lower rate of evaporation was used with the meteorological data to calculate the net surface heat flux, the flux became positive into the ocean (+20 to +50 W m^{-2}), in agreement with the heat transport estimates (Bray, 1988).

In sum, the three major reasons for the regional difference in the heat gain are: (1) T_a-T_s in Matsukawaura is higher than Ishinomaki, (2) wind speed of Ishinomaki is about twice that of Matsukawaura, and (3) offshore conditions have more impact in the southern region than the north.

2) Heat Flux

The local time change of the heat content H in a water column with unit surface area is given by

$$\frac{\partial H}{\partial t} = \rho C_p \int_{-D}^{0} \frac{\partial T}{\partial t} dz = Q + F \qquad (1)$$

where ρ is the density of water, C_p the specific heat under constant pressure, D the thickness of the water column, T the temperature and z is the vertical coordinate taken as positive upward from the sea surface. F is the heat convergence in the sea caused by horizontal advection and/or horizontal mixing, and is given by (Kurasawa *et al.*, 1983)

$$F = -\rho C_p \int_{-D}^{0} \{\nabla \cdot vT + \nabla \cdot \overline{v'T'}\} dz + Q_{-D} \qquad (2)$$

where ∇ is the horizontal gradient operator and $Q_{-D} = \rho C_p \overline{w'T'}|_{z=-D}$ is the heat flux through the bottom of the column, T and the water velocity v are the time

averaged values for the time scale considered, and the prime indicates the temporal fluctuation.

In order to calculate the heat budget for the entire basin of Sendai Bay, we integrate eq. (1) for the area within the bay as shown in Figure 1. The mouth of the bay is taken to be the line connecting Matsukawaura and Kinkazan, and the total volume and surface area are 5.7×10^{10} m^3 and 1.757×10^9 m^2, respectively. In the present study, on the assumption that $Q_D \cong 0$, F is derived from Q and H, and H is estimated from vertical profiles of temperature and salinity for Sendai Bay in 1995. By comparing Q with F, we can find which process, air-sea heat flux or heat convergence in the sea, is more important in the heat balance of the surface layer.

Time series of the monthly mean values in H, Q, and F are shown in Figure 7. It is clear from the figure that from June to September and in January, H is dominated by Q, while during February, April and October to December, it is dominated by F, and Q and F are almost equal contribution in other months. This implies that dependence of H on Q and F varies seasonally. As a result, it is shown that during spring and winter the temporal behaviors of SSTs in the bay can be caused by both Q and F.

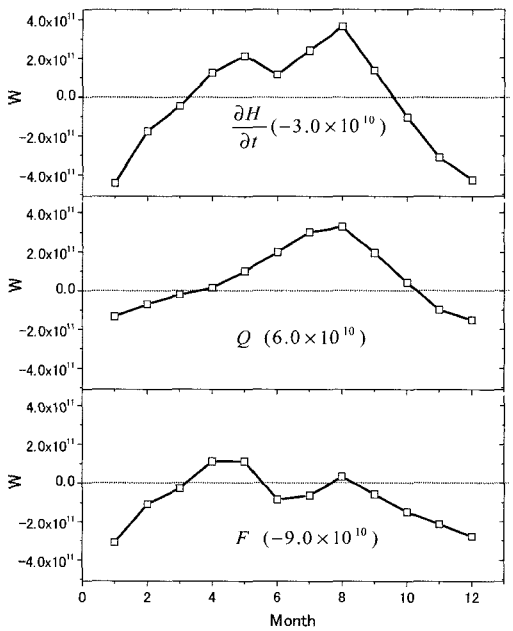

Fig. 7. Heat budget of the Sendai Bay: H, temporal change rate of heat content; Q, net air-sea heat flux; F, oceanic advection. Numeral in the parenthesis of index indicates the annual average (W).

The temporal behaviors of the heat content and advection components are similar to those obtained by Yagi *et al.* (1996) for the coasts of the northeast Japan. In the calculation of surface heat flux, however, one of many problems is that landside data were used instead of open ocean data. For example, if wind speed is increased by 20%, Ishinomaki loses heat to the atmosphere on an annual average (-5.6 Wm^{-2}): the Ishinomaki station is about 2km from the coast, suggesting that open ocean heat flux may be lower than predicted because of higher wind away from the coast. In the next section, we examine the influence of offshore conditions using satellite images.

4. Offshore Conditions

1) General Characteristics in the Kuroshio/Oyashio Frontal Region

The annual mean and standard deviation images shown in Fig. 8, are derived by monthly composite images of AVHRR SST from November 1994 to October 1998. The temporal mean image of the 4-year sequence (left, Figure 8) shows a strong north-south SST gradient. The front is generated by the Kuroshio, Oyashio and Tsugaru Warm Currents, and its shape seems like the character 'U' in the upper part, because temperature in both sides of the figure is warmer than in the vertical center area. The position of the front shifts northward or southward monthly. From the viewpoint of coastal SST environment, it is found that SST distribution is divided into two parts

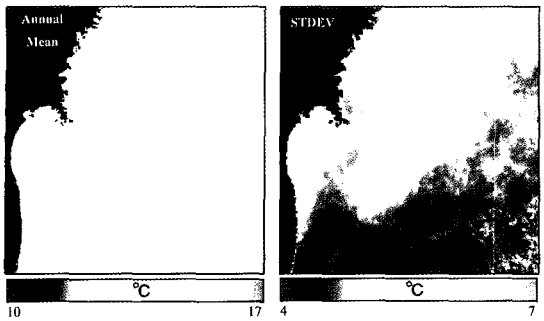

Fig. 8. Images of annual mean (left panel) and standard deviation (right) of AVHRR SST from November 1994 to October 1998.

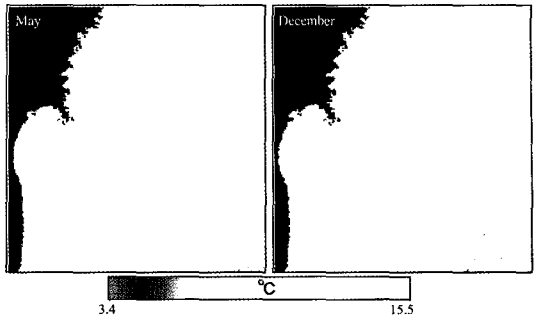

Fig. 9. Monthly mean images of AVHRR SST for the months of May and December during 1990-1994.

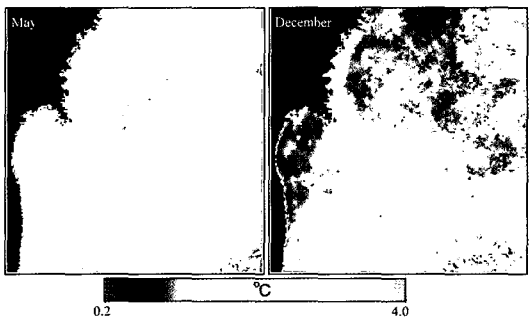

Fig. 10. Images of standard deviation of AVHRR SST for the months of May and December during 1990-1994.

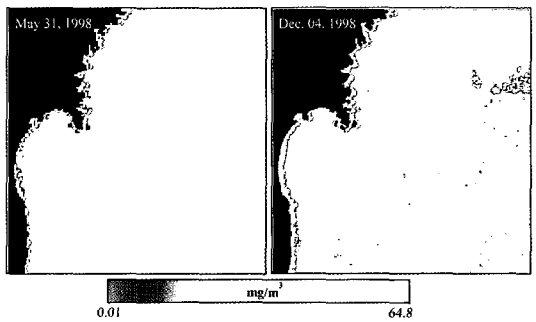

Fig. 11. Chlorophyll-a images of SeaWiFS for the months of May and December, 1998.

centering around the Ojika Peninsula.

From the standard deviation image (Figure 8), it is found that SST variability in Sendai Bay and in the northeastern ocean of the bay is very high. The other areas represent comparatively low seasonal variation, especially from the Ojika Peninsula to Sanriku Coast.

2) Offshore Variation in Spring and Winter

Figures 9 and 10 show the monthly mean and variance images of AVHRR SST in the months of May and December from 1990 to 1994. It is shown that in May, since the southward flowing Oyashio encounters the northward flowing Kuroshio, there is a strong fluctuation of SST along 37-39°N, especially in the offshore region. The Kuroshio also tends to invade the bay due to the strong Oyashio. Southward penetration of the First Oyashio Intrusion off the Sanriku Coast in spring through summer strongly influences various aspects of sea conditions (Hanawa, 1983). Most studies have suggested the Oyashio water system penetrates southward in late winter to spring and goes back northward in autumn based on in-situ temperature data (Sekine, 1988).

Distribution in December, on the contrary, shows that since the Oyashio is very weak, the Tsugaru Warm Current and Kuroshio appear there, but do not have a clear flow pattern. It is clear that SST variance of December is very low as compared to May (Figure 10). In the bay and Sanriku Coast, standard deviation is below 1°C, as represented by blue tones in Figure 10. It suggests that December's offshore condition is more stable than May's.

At Eno Island, the increasing rate of spring CSST is lower because of the Oyashio flowing southward

along the Ojika Peninsula, while in winter the decreasing rate is also the lowest because Eno Island is mainly influenced by the Kuroshio and Tsugaru Warm Current. Based on monthly mean values of the meteorological data from 1994 to 1998, it is shown that fluctuations in the spatially averaged SSTs of images represent a strong seasonal cycle and are highly correlated with fluctuations in the CSSTs; 0.98 for Tashiro Island station and 0.96 for Eno Island.

The characteristics of chlorophyll-a images shown in Figure 11 are similar to those of SST distribution. The image shown in left panel of Figure 11 represents the flow pattern of the Kuroshio, with low chlorophyll-a concentration. The warm water mass flows northward near the bay and turns to the northeast as a form of streamer. In December, however, the Tsugaru Warm Current and Kuroshio dominate this region, but do not extend their influence into Sendai Bay. As shown in SST images, therefore, the bay keeps stable condition due to the peninsula and two warm currents are influential in the area of the Sanriku Coast. As a result, during spring and winter the bay show high SST increase and decrease rate, respectively.

5. Results and Conclusions

In this study, we first examined the SST variability in and around Sendai Bay and investigated its cause from two standpoints; (1) atmospheric forcing in seasonal cycle of meteorological components and heat flux, (2) offshore influence by the Kuroshio, Oyashio, and Tsugaru Warm Current. The seasonal variation in CSST is stronger in Sendai Bay than in the others and the temporal behaviors of CSST at three stations are distinctly changed with a season. The intrusion of the Kuroshio or Oyashio has been suggested as an important contributor to SST variability in the bay (e.g., Nagata *et al.*, 1978). Our analysis suggests that both net air-sea heat flux (Q) and oceanic advection contribute to the seasonal heat budget for the bay.

Temporally averaged SST and coastal meteorological data in 1995 have been used to estimate daily and monthly mean surface heat fluxes in Sendai Bay. The spatial pattern of the sensible heat flux and in turn the net surface heat flux is directly reflected by those of T_a-T_s and wind in Sendai Bay. The magnitude of the net surface heat flux increases with distance from the coast as T_a-T_s and wind speed become larger. The lowest heat gain (35 W m^{-2}) occurs in the northern region, where SSTs are least influenced by cold water from the offshore. In all net surface heat fluxes, the bay gains heat from the atmosphere on an annual average, but only in winter loses heat to the atmosphere.

In the calculation of heat flux and satellite images, it is shown that during spring and winter both Q and F can cause the temporal behaviors of SSTs in the bay. As a result, it can be said that the peninsula plays a role differentiating the bay from Eno Island, which during winter shows higher SST than the bay.

Acknowledgments

This work was supported by the Basic Research Project, "Development of Restoration Technologies for the Polluted Estuary" of KORDI and the Public Benefit Project of Remote Sensing, "Satellite Remote Sensing for Marine Environment" of Korea Aerospace Research Institute.

References

Bray, N. A., 1988. Thermohaline circulation in the

Gulf of the California, *J. Geophys. Res.*, 93(C5): 4993-5020.

Bunker, A. F., 1976. Computations of surface energy flux and annual air-sea interaction cycles of the North Atlantic Ocean, *Mon. Weather Rev.*, 104: 1122-1140.

Castro, R., M. F. Lavin, and P. Ripa, 1994. Seasonal heat balance in the Gulf of California, *J. Geophys. Res.*, 99(C2): 3249-3261.

Friehe, C. A., and K. F. Schmitt, 1976. Parameterization of the air-sea interface fluxes of sensible heat and moisture by the bulk aerodynamic formulas, *J. Phys. Oceanogr.*, 6: 2035-2060.

Gill, A. E., 1982. *Atmosphere-Ocean Dynamics*, 662 pp., Academic Press, San Diego, Calif.

Hanawa, K., 1983. Sea surface temperature off Sanriku coast and east of Tsugaru Strait monitored by ferry Ishikari (I) 1981, *Tohoku Geophys. J. (Sci. Rep. Tohoku Uni., Ser. 5)*, 29(3): 129-149.

Hanawa, K., 1995. Southward penetration of the Oyashio water system and the wintertime condition of midlatitude westerlies over the North Pacific, *Bull. Hokkaido Natl. Fish. Res. Ins.*, 59: 103-120.

Iwasaka, N. and K. Hanawa, 1990. Climatologies of marine meteorological variables and sea fluxes in the North Pacific computed from COADS, *Tohoku Geophys. J. (Sci. Rep. Tohoku Uni., Ser. 5)*, 33(3): 185-239.

Jones, I. S. F., Y. Sugimoto, and R. W. Stewart, (Eds.), 1993. *Satellite Remote Sensing of the Oceanic environment*, 523 pp., Seibutsu Kenkyusha, Tokyo.

Kizu, S., 1998. Systematic errors in estimation of insolation by empirical formulas, *J. Oceanogra.*, 54: 165-177.

Kurasawa, Y., K. Hanawa, and Y. Toba, 1983. Heat balance of the surface layer of the sea at ocean weather station T, *J. Oceanogr. Soc. Japan*, 20: 255-263.

Lavin, M. F. and S. Organista, 1988. Surface heat flux in the northern Gulf of California, *J. Geophys. Res.*, 93(C11): 14,033-14,038.

Nagata, Y., Y. H. Sakurai, T. H. Teramoto, K. N. Sekino, and Date, T. K., 1978. Regional properties of surface temperature at Sanriku Coast, *Bull. On coastal ocean.*, 16(1): 43-49. (In Japanese)

Oceanographic Society of Japan, 1985. *Coastal Oceanography of Japanese Islands*, 1,105 pp., Tokai Uni. Press, Tokyo.

Paden, C. A., C. D. Winant, and M. R. Abbott, 1993. Tidal and atmospheric forcing of the upper ocean in the Gulf of California, 2, Surface heat flux, *J. Geophys. Res.*, 98(C11): 20,091-20,103.

Reed, R. K., 1977. On estimating insolation over the ocean, *J. Phys. Oceanogr.*, 7: 482-485.

Reed, R. K., 1983. Heat fluxes over the eastern tropical Pacific and aspects of the 1972 El Niño, *J. GeopPhys. Res.*, 88(C14): 9627-9638.

Sekine, Y., 1988. Anomalous southward intrusion of the Oyashio east of Japan, 1, Influence of the seasonal and interannual in the winter stress over the North Pacific, *J. Geophys. Res.*, 93: 2247-2255.

Yagi, H., K. T. R. Ogata, T. R. Sakamoto, and K. O. Nadaoka, 1996. SST variability at open coastal region during summer, in *Proceedings of Coastal Engineering*, JSCE, 43: 1201-1205 (In Japanese).

Yang, C. S., H. Tanaka, M. Sawamoto, and K. Hanawa, 1999a. Influence of off-shore oceanic condition and weather variation on the surface thermal condition in and around

Sendai Bay, in *Proceedings of Coastal Engineering*, JSCE, 46: 1326-1330 (In Japanese).

Yang, C. S., H. Tanaka, M. Sawamoto, and K. Hanawa, 1999b. Empirical orthogonal function analysis of Advanced Very High Resolution Radiometer sea surface temperature variability over the Northwest Pacific, in *Progress in Coastal Engineering and Oceanography*, edited by B.H. Choi, Hanrimwon Publishing Co., Seoul, 2: 131-142.

Yang, C. S., 2000. Variability of sea surface temperature in the heating period at the coastal area of the northeast Japan, *Annual J. Hydraulic Eng.*, JSCE, 44: 927-932 (In Japanese with English abstract).

Yang, C. S., 2000. Atmospheric and oceanic forcings on the spring coastal thermal environment in the Kuroshio/Oyashio Frontal Region, *Coastal Eng. J.*, 4(42): 407-425.

Yang, C. S., H. Tanaka, M. Sawamoto, and K. Hanawa, 2000. Estimation of the thermal environmental around Sendai Bay, in *Proceedings of Civil Engineering in the Ocean*, JSCE, 47: 135-140.

Yang, C. S., H. Tanaka, M. Sawamoto, and K. Hanawa, 2001. Long-term mean environment of sea water temperature in Sendai Bay and the adjacent area based on SVD and heat budget analysis, in *Proceedings of Civil Engineering in the Ocean*, JSCE, 48: 1456-1460 (In Japanese).

Appendix: Surface Heat Flux Formulas

The net surface heat flux Q is the sum of the net solar (or short-wave) radiation Q_s, the net long-wave radiation Q_b, the latent heat flux Q_e and the sensible heat flux Q_h:

$$Q = Q_s + Q_b + Q_e + Q_t \quad \text{(A1)}$$

Fluxes into the sea are positive, and those out of it are negative.

The net solar radiation Q_s is given by (Reed, 1977):

$$Q_s = Q_o(1 - 0.62C + 0.0019\alpha)(1 - A) \quad \text{(A2)}$$

where Q_o (W m^{-2}) is the clear-sky mean daily insolation. The (1-A) term introduces the effect of reflection, with albedo A = 0.06 (Payne, 1972). The first set of parenthesis in (A2) includes the effect of the clouds (C is the cloud cover in tenths) and that of the altitude of the sun from the horizontal at noon (α, in degrees). A little geometry shows that

$$\alpha = 90° - L + \delta - \eta \quad \text{(A3)}$$

where δ = 23.87sin[2π(t-82)/365] is the Sun's declination, L is the latitude in degrees, and $\eta < 0.002°$ (the angle subtended by the Earth radius, seen from the Sun) and can be neglected. Q_o is calculated analytically with the Smithsonian formulae:

$$Q_o = A_0 + A_1\cos\phi + B_1\sin\phi + A_2\cos 2\phi + B_2\sin 2\phi \quad \text{(A4)}$$

where ϕ = (2π/365)(t-21), where t is the Julian day. For the coefficients in this formula we used the values given by Reed (1977) for the latitude band 20°S to 40°N:

$$\begin{aligned} A_0 &= -15.82 + 326.87\cos L \\ A_1 &= 9.63 + 192.44\cos(L + 90°) \\ B_1 &= -3.27 + 108.70\sin L \\ A_2 &= -0.64 + 7.80\sin 2(L - 45°) \\ B_2 &= -0.50 + 14.42\cos 2(L - 5°) \end{aligned} \quad \text{(A5)}$$

The net longwave or back radiation was computed with the expression (Reed, 1983):

$$Q_b = -\sigma\varepsilon(T_s + 274)^4(0.254 - 0.00495e_a)(1 - 0.8C) \quad \text{(A6)}$$

where T_s (in degrees Celsius) is the sea surface temperature, $\sigma = 5.67 \times 10^{-8}$ W m^{-2} K^{-4} is the Stefan-Boltzman constant, and ε = 0.97 is the emissivity of the sea surface.

The water vapor pressure of air e_a (in millibars) was calculated as $e_a = (H/100)e_s$, where H (percentage) is the relative humidity, and e_s is the saturation water vapor pressure at the sea surface, assuming saturation at T_s (Gill, 1982):

$$e_s = 0.98[1 + 10^{-6} P(4.5 + 0.0006T_s^2)]10^{\gamma} \quad \text{(A7)}$$

where, $\gamma = (0.7859 + 0.03477T_s)/(1 + 0.00412T_s)$ and P is atmospheric pressure in millibars.

The latent and sensible heat fluxes are estimated using the bulk aerodynamic formulas. The latent heat flux is (Gill, 1982)

$$Q_e = -\rho_a C_e W(q_s - q_a)L_v \quad \text{(A8)}$$

where ρ_a is the air density and was taken from Iwasaka and Hanawa (1990), C_e is an exchange coefficient, W is the mean wind speed in meters per second, q_s is the saturation specific humidity of the sea surface, q_a is the specific humidity of air and the latent heat of evaporation $L_v = (2.5008 \times 10^6) - (2.3 \times 10^3)T_s \mathrm{Jkg}^{-1}$ (Gill, 1982). These specific humidities were calculated with (Gill, 1982)

$$\begin{aligned} q_s &= (0.62197e_s)/(P - 0.378e_s) \\ q_a &= (0.62197e_a)/(P - 0.378e_a) \end{aligned} \quad \text{(A9)}$$

The value of C_e depends on wind speed and atmospheric stability and was taken from Table 4 in Bunker (1976).

The sensible heat flux was calculated as (Friehe and Schmitt, 1976)

$$\begin{aligned} Q_t &= -\rho_a C_p(0.0026 + 0.86 \times 10^{-3} W\Delta T) && W\Delta T<0 \\ Q_t &= -\rho_a C_p(0.002 + 0.86 \times 10^{-3} W\Delta T) && 0<W\Delta T<25 \\ Q_t &= -\rho_a C_p(1.46 \times 10^{-3} W\Delta T) && W\Delta T>25 \end{aligned} \quad \text{(A10)}$$

where ($\Delta T = T_s - T_a$) and C_p is the specific heat of air at constant pressure

$$C_p = 1004.6(1 + 0.8375q_a)Jkg^{-1}K^{-1} \quad \text{(A11)}$$